Scientific Reports

https://doi.org/10.1038/s41598-026-39715-w

Article in Press

Cadmium exposure induces renal fibrosis by inhibiting hsa_circ_0075684/miR-363-3p/KLF4 signaling pathway

Received: 28 May 2025

Accepted: 6 February 2026

Published online: 13 February 2026

Cite this article as: Zhou J., Huang Y., Li G. *et al.* Cadmium exposure induces renal fibrosis by inhibiting hsa_circ_0075684/miR-363-3p/KLF4 signaling pathway. *Sci Rep* (2026). https://doi.org/10.1038/s41598-026-39715-w

Jiazhen Zhou, Yiqi Huang, Guoliang Li, Zhiqiang Zhao, Yaotang Deng, Siming Xian, Yue Hu, Mushi Yi & Lili Liu

Cadmium exposure induces renal fibrosis by inhibiting hsa_circ_0075684/miR-363-3p/KLF4 signaling pathway

Jiazhen Zhou[a#], Yiqi Huang[b#], Guoliang Li[a], Zhiqiang Zhao[a], Yaotang Deng[a], Siming Xian[a], Yue Hu[a], Mushi Yi[a], Lili Liu[a*]

[a] Department of Toxicology, Guangdong Province Hospital for Occupational Disease Prevention and·Treatment, Guangzhou, 510300, China

[b] Guang Zhou Haizhu Maternity and Child Health Hospital, Guang Zhou 510240, China

[#] These authors have contributed equally to this work.

[*] Correspondence Author: Lili Liu, Department of Toxicology, Guangdong Province Hospital for Occupational Disease Prevention and·Treatment, Guangzhou, 510300, China. Tel: 020-34063151, Fax: 020-34063151. E-mail: lli257@163.com. ORCID□0000-0001-7733-7654.

Abstract

To date, no effective chelation therapy exists to remove cadmium (Cd) from the kidneys, a condition that increases the risk of cadmium-induced chronic kidney disease among humans. consequently, it is vital to prevent kidney damage due to cadmium exposure. However, it has been challenging to identify an early diagnostic marker of cadmium-induced kidney damage through mechanism studies. Interestingly, our previous study revealed that the expression of the microRNA miR-363-3p was upregulated in workers who had been diagnosed with chronic occupational cadmium toxicity. Thus, we aimed to investigate the role of miR-363-3p and its potential signaling pathway in cadmium-induced kidney damage. In this study, we identified a novel signaling pathway, hsa_circ_0075684/miR-363-3p/Kr ü ppel-Like Factor 4 (KLF4), through a comprehensive bioinformatics analysis involving six databases. Next, we validated the role of the hsa_circ_0075684/miR-363-3p/KLF4 pathway in human renal tubular epithelial cell line (HK-2) treated with 0, 5, 10 and 15 μM cadmium chloride ($CdCl_2$). Reverse transcription quantitative PCR (RT-qPCR) and western blot analyses showed that cadmium exposure induced renal fibrosis by regulating the expression of classic renal fibrosis biomarkers, including Fibronectin (Fn), E-cadherin (E-cad) and □-smooth muscle actin (□-SMA) through hsa_circ_0075684/miR-363-3p/KLF4 pathway inhibition. In a mice subchronic model (treated with 0, 5, 10 and 20 mg/kg $CdCl_2$), Masson's staining revealed obvious renal fibrosis in mice treated with 5, 10 and 20 mg/kg $CdCl_2$ compared to the control group. The altered expression of hsa_circ_0075684/miR-363-3p/KLF4 pathway components and classic renal fibrosis biomarkers in model mice exposed to cadmium was consistent with that observed in HK-2 cells. In summary, we first report hsa_circ_0075684/miR-363-3p/KLF4 axis in cadmium nephrotoxicity, positioning it as a potential early diagnostic marker for cadmium-induced renal fibrosis.

Keywords: hsa_circ_0075684/miR-363-3p/KLF4; cadmium; renal fibrosis; circular RNA

Abbreviations

Abbreviations	Full term
Cd	cadmium
CdCl2	cadmium chloride
RT-qPCR	Reverse transcription quantitative PCR
Fn	Fibronectin
E-cad	E-cadherin
□-SMA	□-smooth muscle actin
CKD	chronic kidney disease
PI3K	phosphoinositide 3-kinase
CTD	Comparative Toxicogenomics Database
GTEx	Genotype-Tissue Expression
circRNA	circular RNA
MYLIP	myosin regulatory light chain interacting protein
GO	Gene Ontology
KEGG	Kyoto Encyclopedia of Genes and Genomes
KLF4	Krüppel-Like Factor 4
ANP32E	Acidic Nuclear Phosphoprotein 32 Family Member E
COL1A2	Collagen Type I Alpha 2 Chain
ITGA5	Integrin Subunit Alpha 5
UTRs	untranslated regions
WT	wilde type
MUT	mutant
TPM	Transcripts per million

Introduction

Cadmium, which exists mainly as Cd^{2+}, is a toxic heavy metal that can enter the human body through the gastrointestinal and respiratory tracts [1]. Cadmium exposure damages the urinary, digestive, skeletal, respiratory, cardiovascular and reproductive systems [2,3]. The biological half-life of cadmium in the human body is 16–30 years[4], enabling its accumulation in organs, and nearly half of the cadmium taken up by the body accumulates in the kidneys, leading to chronic kidney disease (CKD; i.e., chronic renal insufficiency)[5,6]. In the last two decades, approximately 697.5 million cases of CKD were reported worldwide, among which about 20% were reported in China GBD Chronic Kidney Disease [7]. By 2020, the all-age rate of death due to CKD nearly doubled, and the all-age prevalence increased by 30% to 700 million people worldwide [8]. In summary, cadmium exposure poses a huge threat to human health, but no effective cure is available. Thus, in-depth research on the mechanism by which cadmium exposure induces CKD is urgently needed.

In our previous study, we found that expression of the microRNA (miRNA) miR-363-3p was upregulated in workers who had been diagnosed with chronic occupational cadmium poisoning as of 2004 and continued to exhibit renal insufficiency (urinary β2-microglobulin and retinal-binding protein concentrations higher than the thresholds included in China's national diagnostic criteria) in 2015, more than 10 years after treatment [9]. We further found that miR-363-3p could promote apoptosis by downregulating phosphoinositide 3-kinase (PI3K) expression in human renal epithelial cells exposed to cadmium [9]. However, miR-363-3p is multifunctional and may not uniquely lead to CKD in cadmium-exposed workers [10-12]. Renal fibrosis is a common pathological feature of all types of end-stage CKD [13]. Long-term cadmium exposure alters the expression of fibrosis markers, activates the renal epithelial–mesenchymal transition and induces histopathological changes associated with fibrosis [14,15].

MiR-363-3p was also found to inhibit the expression of renal fibrosis markers in TGF-β1-treated cells by targeting TGF-β2, suggesting an association of this miRNA with renal fibrosis [16]. Based on the above research background, in this study, we hypothesised that miR-363-3p may play an important role in cadmium-induced renal fibrosis.

Generally, we can identify potential signal pathway related with miR-363-3p by using analytical approaches such as genomics, transcriptomics and proteomics. Although such approaches are very helpful, they are costly and time-consuming. For reducing costs, we have focused on bioinformatics as an efficient approach. The development of bioinformatics analyses has enabled researchers to predict the biomarkers and potential mechanisms of action of diseases quickly and efficiently; accordingly, researchers are increasingly using bioinformatics analyses to predict the regulatory networks of diseases [17-19]. Thus, to predict a new regulatory signal pathway, in this study we conducted bioinformatics analyses involving six databases (miRDB [20], miRWalk [21], TarBase [22], starBase [23], the Comparative Toxicogenomics Database (CTD)[24] and Genotype-Tissue Expression (GTEx))[25] and three key words (cadmium, kidney and miRNA-363-3p). Three classic miRNA databases (miRDB, miRWalk, TarBase) were used for prediting target genes with key words miRNA-363-3p; StarBase is a database for predicting potential upstream of miR-363-3p; CTD is a robust, publicly available database that provides manually curated information about chemical-gene/protein interactions, chemical-disease and gene-disease relationships [24], which can identify targets for cadmium; GTEx provides a tissue-specific gene bank [25] that is helpful for searching targets from kidney. Ultimately, we identified a new signaling pathway, hsa_circ_0075684-miRNA-363-3p-KLF4, with a potential role in cadmium-induced CKD.

One component of this predicted signaling pathway is KLF4, which was first discovered in 1996. This zinc-finger transcription factor family member is

involved in processes such as cell proliferation, differentiation, apoptosis and embryonic development [26,27]; it also has been shown to inhibit fibrogenesis [27,28]. Moreover, KLF4 was found to be nephroprotective [29,30], possibly due to its inhibition of renal inflammation or the proliferation and differentiation of vascular endothelial cells to resist fibrosis, or its negative regulation of renal epithelial-mesenchymal transition and fibrosis [27,31-33]. Another crucial molecule in the predicted signaling pathway, the circular RNA (circRNA) hsa_circ_0075684, was identified through bioinformatics analysis; but we were unable to find relevant information about it or hsa_circ_0131240 or their host gene, myosin regulatory light chain interacting protein (MYLIP), from previous research. However, previous studies found that many circRNAs play a role in renal fibrosis by adsorbing miRNAs but no novel study in recent 3 years: for example, the circ-ITC/miR-33a-5p/SIRT6 signaling axis was shown to attenuate renal fibrosis in mice with streptozotocin-induced diabetes [34], and circPlekha7 was shown to inhibit renal fibrosis by targeting the miR-493-3p/KLF4 axis to inhibit the epithelial-mesenchymal transition and fibrosis in renal tubular epithelial cells [35]. Based on the above research background, we hypothesise that hsa_circ_0075684 acts as a sponge to adsorb miRNA-363-3p and thus plays an important role in cadmium-induced renal fibrosis, ultimately leading to CKD.

In summary, in this study we investigated the role of miR-363-3p in cadmium exposure-induced renal fibrosis and the underlying mechanism. The study was conducted in two parts: in the first part, we conducted a bioinformatics analysis to screen for miR-363-3p related signaling pathways. In the second part, we proved that the predicted hsa_circ_0075684/miR-363-3p/KLF4 signaling pathway plays a role in cadmium-induced renal fibrosis via *in vitro* and *in vivo* experiments. Our findings provide a new direction for searching target through bioinformatics analysis and suggest a potential biomarker for the early diagnosis of cadmium-induced renal fibrosis.

Results

Bioinformatics prediction of genes targeted by miR-363-3p and experimental validation in a model of cadmium-induced fibrosis in human renal tubular epithelial cells

To quickly identify target genes downstream of miR-363-3p, we searched the miRDB, miRWalk and TarBase databases and respectively obtained 922, 8169 and 336 mRNAs with potential binding sites for miR-363-3p (Supplementary Table 2). Intersecting the prediction results from the three databases yielded 102 genes with potential miR-363-3p binding sites (Supplementary Table 3 and Supplementary Figure 1). Gene Ontology (GO) enrichment analysis revealed that these 102 genes were mainly associated with the regulation of cytoplasmic translation and elongation, the modulation of cellular responses to misfolded proteins, Golgi compartments, integrin complexes and actinoglobulin (Supplementary Figure 2a). Kyoto Encyclopedia of Genes and Genomes (KEGG) enrichment analysis showed that these miR-363-3p target genes were mainly enriched in the extracellular matrix and PI3K signaling pathways (Supplementary Figure 2b). Subsequently, cadmium-related genes were identified using the CTD database, which yielded 929 genes that had been experimentally verified as associated with cadmium and whose expression was downregulated following after cadmium treatment (Supplementary Table 4). We then used the GTEx database to identify 16,358 kidney-related genes (Supplementary Table 5). We used the R software package 'VennDiagram' to intersect the predicted genes downstream of miR-363-3p (102 genes), cadmium-related genes (929 genes) and kidney-related genes (16358 genes), which yielded four genes: Acidic Nuclear Phosphoprotein 32 Family Member E (*ANP32E)*, Kr ü ppel-Like Factor 4 (*KLF4)*, Collagen Type I Alpha 2 Chain (*COL1A2)* and Integrin Subunit Alpha 5 (*ITGA5)*, as shown in Figure 1a.

Subsequently, we used the starBase database to predict circRNAs that regulate miR-363-3p. Finally, we selected hsa_circ_0075684 according to the maximum number of Clip-seq experiments, as shown in Table 1.

To investigate the mechanism of cadmium-induced renal fibrosis, we used the CCK-8 assay to determine the appropriate concentration of cadmium for exposure. The results showed that after 48 h, the viability of HK-2 cells decreased with increasing $CdCl_2$ concentration, as shown in Figure 1c. Therefore, we chose the cadmium exposure concentration associated with approximately 80% cell viability as the highest exposure concentration and created four treatment groups: 0, 5, 10 and 15 μM. We found that the expression of the pro-fibrotic proteins Fn and α-SMA were upregulated and that of the anti-fibrotic protein E-Cad was downregulated at all $CdCl_2$ concentrations, and there was a statistically significant dose–response relationship (β_{Fn}/95%confidence = 0.046/0.032 to 0.059, $\beta_{E\text{-}Cad}$/95%confidence = -0.042/-0.052 to -0.031, $\beta_{\alpha\text{-}SMA}$/95%confidence = 0.046/0.027 to 0.065, all $P < 0.05$, Figure 1e and 1f). This suggests that cadmium exposure can induce fibrosis in renal tubular epithelial cells.

Based on our previous results, we next used RT-qPCR to examine the expression of miR-363-3p in HK-2 cells treated with different cadmium concentrations for 48 hours [9]. The results showed that the expression of miR-363-3p increased gradually as the cadmium exposure concentration increased ($P < 0.05$, Figure 1d). This suggests that cadmium-induced fibrosis in renal tubular epithelial cells is associated with the upregulation of miR-363-3p expression. Through a bioinformatics analysis, we identified four genes associated with miR-363-3p, cadmium and the kidney: *ANP32E*, *COL1A2*, *KLF4* and *ITGA5*. We then examined the expression of these four genes. We found that the expression of KLF4 decreased after treating HK-2 cells with different cadmium concentrations for 48 h, and this dose–response relationship was significant (β_{KLF4}/95%confidence = -0.023/-0.032 to -0.015, $P < 0.05$, Figure 1d-1f), while

with no significance with ANP32E, COL1A2 and ITGA4 (not presented in the study). We also examined the expression of screened target genes upstream of miR-363-3p and found that the expression of hsa_circ_0075684 decreased as the cadmium concentration increased within a certain range, and this relationship was also statistically significant ($P < 0.05$, Figure 1d). These findings suggested that the hsa_circ_0075684/miR-363-3p/KLF4 signal pathway (Figure 1b) might be involved in regulating cadmium-induced renal fibrosis.

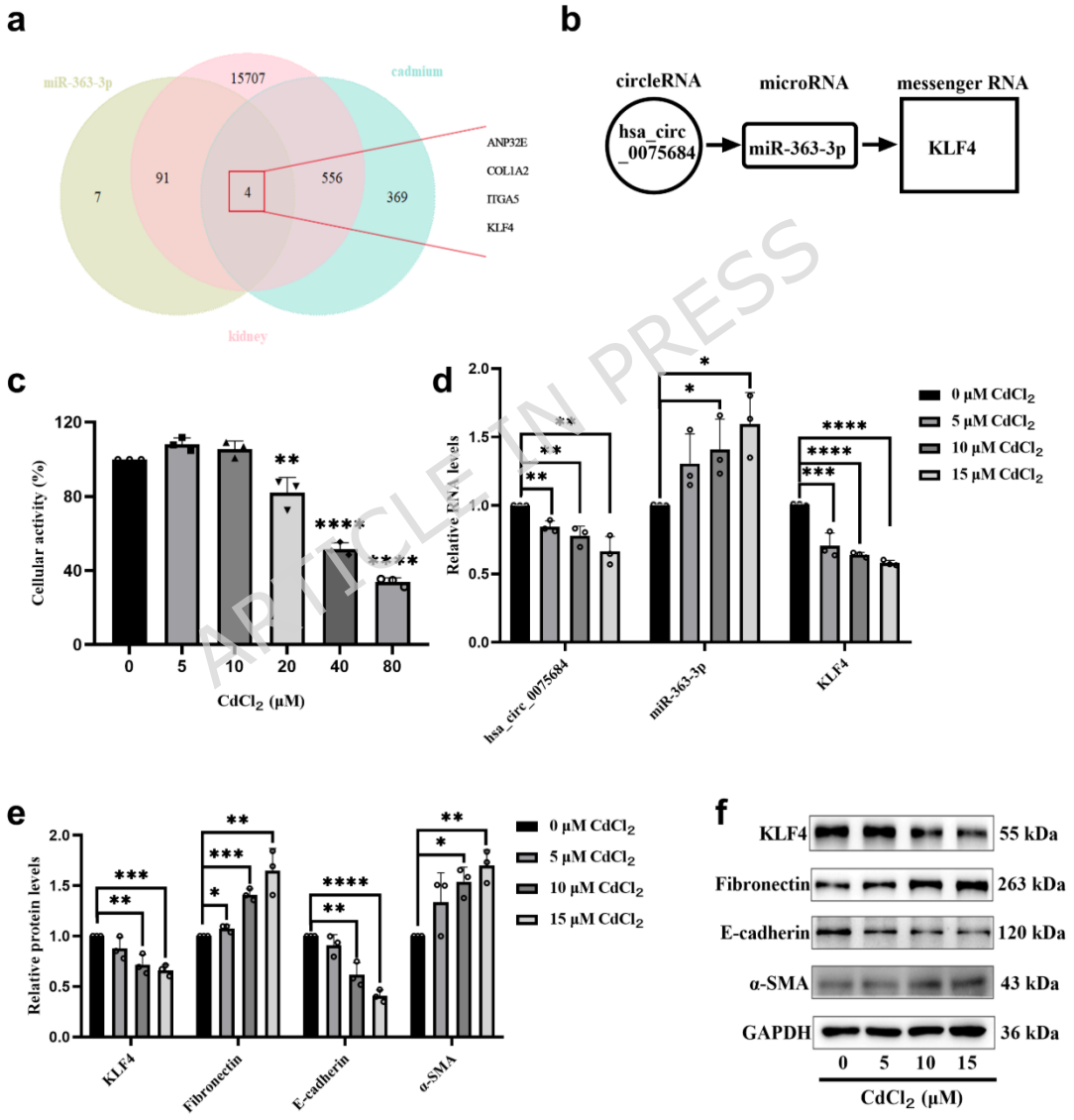

Figure 1. A new signal pathway hsa_circ_0075684/miR-363-3p/KLF4 detected by bioinformatics analysis and experimental validation. (a) Venn

diagram of the intersection of genes associated with miR-363-3p, cadmium and the kidney. (b) A potential signal pathway hsa_circ_0075684/miR-363-3p/KLF4 predicted by bioinformatics analysis. (c) Changes in HK-2 cell viability following exposure to cadmium at concentrations of 0-80 μM. (d) Relative RNA expression levels of hsa_circ_0075684, miR-363-3p and KLF4 in HK-2 cells treated with cadmium (0-15 μM). (e, f) Relative protein expression levels of KLF4 and fibrosis-associated proteins in HK-2 cells treated with cadmium (0-15 μM). (n= 3 / each group, * $P < 0.05$, ** $P < 0.01$, *** $P < 0.001$, **** $P < 0.0001$)

MiR-363-3p bound to the 3′-untranslated regions (UTRs) of KLF4 and hsa_circ_0075684

To verify whether miR-363-3p would bind to KLF4 and hsa_circ_0075684, we performed dual-luciferase reporter gene experiments. TargetScan and starBase predictions indicated that the KLF4 3′-UTR and hsa_circ_0075684 3′-UTR might bind to miR-363-3p, and the results are shown in Figure 2b and 2c. The results of the dual-luciferase reporter gene assay showed that treatment with a miR-363-3p mimic (used psiCHECK-2 Vector as shown in Figure 2a) could significantly reduce luciferase activity in both the KLF4 3′-UTR-wild type (WT) and hsa_circ_0075684 3′-UTR-WT groups; while it could not affect the luciferase activity in both the KLF4 3′-UTR-mutant (MUT) and hsa_circ_0075684 3′-UTR-MUT groups (Figure 2d and 2e). In summary, these experimental results indicated that miR-363-3p could regulate KLF4 expression at the post-transcriptional level by binding specifically to the 3′-UTR of KLF4, while hsa_circ_0075684 regulated the expression of downstream genes by adsorbing miR-363-3p.

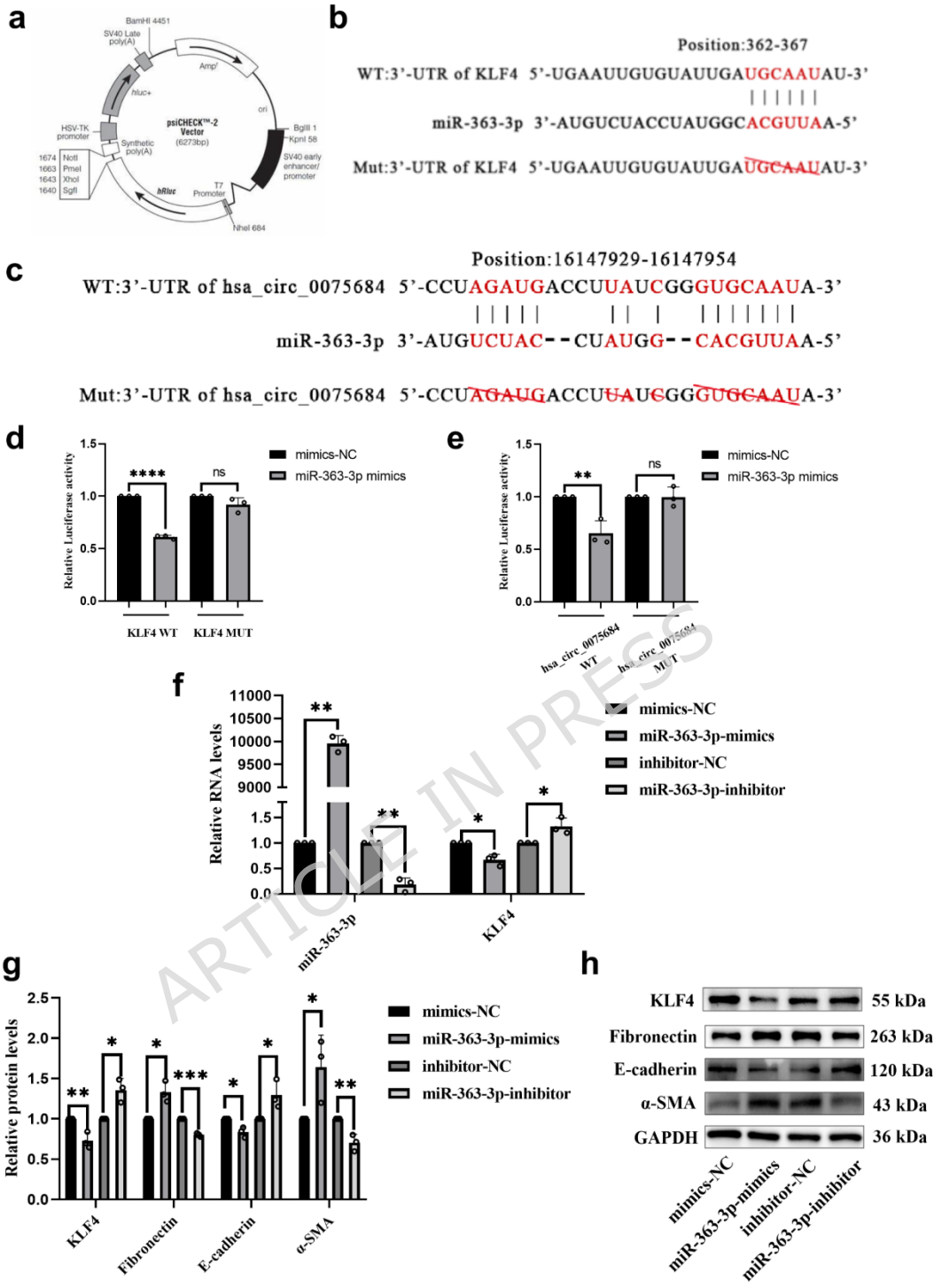

Figure 2. Overexpressing and inhibiting the expression levels of miR-363-3p regulated the expression of KLF4 and fibrosis-associated proteins. (a) Schematic diagram of the psiCHECK™-2 plasmid. (b) TargetScan database prediction of miR-363-3p binding sites in the KLF4 3′-UTR. (c) starBase database

predictions of miR-363-3p binding sites in the hsa_circ_0075684 3′-UTR. (d) Dual-luciferase reporter gene assay to detect the binding of miR-363-3p to the target KLF4 site in HK-2 cells. (e) Dual-luciferase reporter gene assay to detect the binding of miR-363-3p to the target hsa_circ_0075684 site in HK-2 cells. (f) Relative RNA expression levels of miR-363-3p and KLF4 in HK-2 cells under overexpressing or inhibiting the expression levels of miR-363-3p. (g, h) Relative protein expression levels of KLF4 and fibrosis-associated proteins in HK-2 cells under overexpressing or inhibiting the expression levels of miR-363-3p. Each experiment was repeated at least three times. (n= 3 / each group, * $P < 0.05$, ** $P < 0.01$, *** $P < 0.001$, **** $P < 0.0001$, ns: no significant difference)

MiR-363-3p promotes cadmium-induced renal fibrosis through downregulating KLF4

To investigate the regulatory effects of miR-363-3p on KLF4, we established a cell model of miR-363-3p overexpression and inhibition. MiR-363-3p expression was significantly upregulated after 48 h of treatment with miR-363-3p mimics, but significantly downregulated after 48 h of treatment with an miR-363-3p inhibitor ($P < 0.05$, Figure 2f). KLF4 mRNA and protein expression were detected by RT-qPCR and western blotting, respectively, and the results showed that the expression of KLF4 was downregulated in the miR-363-3p mimic-treated group but upregulated in the miR-363-3p inhibitor-treated group, and both differences were significant compared with the corresponding control groups (all $P < 0.05$, Figure 2g and 2h). Meanwhile, western blotting showed that transfection with miR-363-3p mimics promoted the expression of Fn and α-SMA and suppressed the expression of E-Cad, while the reverse expression pattern was observed following transfection with an miR-363-3p inhibitor (all $P < 0.05$, Figure 2g and 2h).

To further elucidate how the regulation of KLF4 expression by miR-363-3p contributes to cadmium-induced renal fibrosis, HK-2 cells were treated with 15 μM cadmium and an miR-363-3p inhibitor for 48 hours. Compared with cells in the cadmium-only treated group, cells in the Cd+miR-363-3p inhibitor group exhibited decreased expression of miR-363-3p and increased mRNA and protein expression of KLF4, and these differences were statistically significant (all $P < 0.05$, Figure 3a- 3c). In addition, the elevated levels of Fn and α-SMA proteins in response to cadmium exposure were reversed in the Cd+miR-363-3p inhibitor group, while the expression of E-Cad protein was increased (all $P < 0.05$, Figure 3b and 3c). In summary, the inhibition of miR-363-3p attenuated cadmium-induced renal fibrosis by upregulating KLF4 expression.

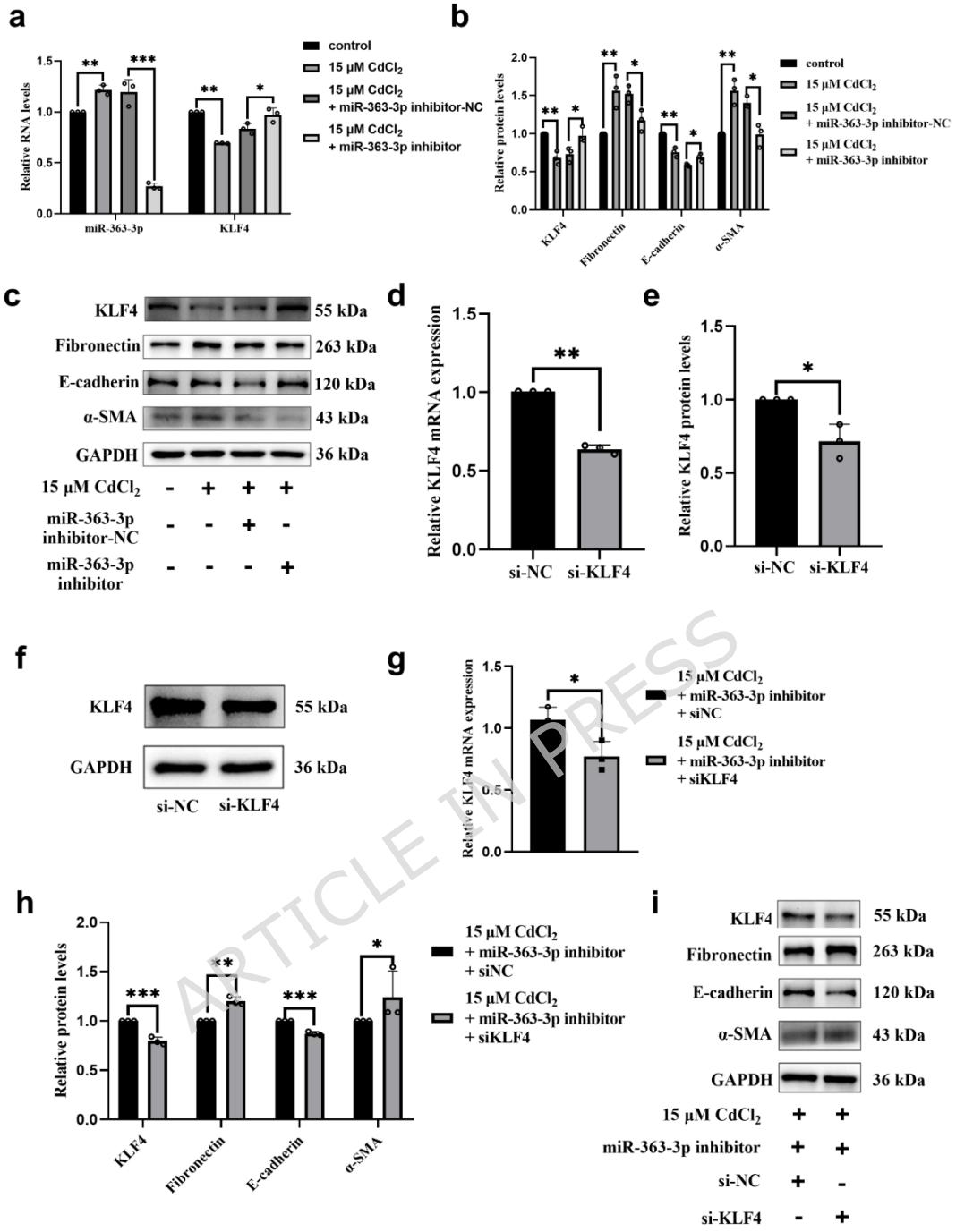

Figure 3. Knockdown of KLF4 and downregulation of miR-363-3p mitigate the expression of miR-363-3p, KLF4 and fibrosis indicators after cadmium treatment. (a) Relative RNA expression of miR-363-3p and KLF4 in HK-2 cells after treatment with 15 μM $CdCl_2$ + miR-363-3p inhibitor. (b, c) Relative protein expression of KLF4 and fibrosis-associated proteins in HK-2 cells after treatment with 15 μM $CdCl_2$ + miR-363-3p inhibitor. (d–f) Relative

expression levels of KLF4 in HK-2 cells after treatment with siKLF4. (g-i) Relative expression levels of KLF4 and fibrosis-related proteins in HK-2 cells after treatment with 15 μM $CdCl_2$ + miR-363-3p inhibitor + siKLF4. Each experiment was repeated at least three times. (n= 3 / each group, * $P < 0.05$, ** $P < 0.01$, *** $P < 0.001$)

To further validate the effect of miR-363-3p on KLF4, a cell model co-transfected with a miR-363-3p inhibitor and si-KLF4 was constructed in this study. First, the KLF4 knockdown efficiency after transfection with si-KLF4 was verified in HK-2 cells, and the results showed that the expression of KLF4 was downregulated (all $P < 0.05$, Figure 3d-3f). Compared with the Cd+miR-363-3p inhibitor+si-NC group, the expression of KLF4 and E-Cad was downregulated and the expression of Fn and α-SMA was upregulated in the Cd+miR-363-3p inhibitor+si-KLF4 group (all $P < 0.05$, Figure 3g-3i). The above results indicated that the mitigating effect of miR-363-3p inhibition on cadmium-induced renal fibrosis could be reversed by knocking down KLF4.

Hsa_circ_0075684 regulates cadmium-induced renal fibrosis via miR-363-3p

To investigate whether hsa_circ_0075684 plays a regulatory role by adsorbing miR-363-3p, we established a cell model of hsa_circ_0075684 overexpression. Figure 4a shows that the cell model was successfully constructed. Compared with the control group, the expression of miR-363-3p was downregulated and the expression of KLF4 was upregulated in the hsa_circ_0075684 overexpression group (all $P < 0.05$, Figure 4a-4c); additionally, the expression of Fn and α-SMA was downregulated and that of E-Cad was upregulated (all $P < 0.05$, Figure 4b and 4c). Subsequently, HK-2 cells were

simultaneously treated with 15 μM cadmium and pLC5-ciR-hsa_circ_0075684 for 48 hours. The results showed that the expression of hsa_circ_0075684 was significantly elevated in the Cd+pLC5-ciR-hsa_circ_0075684 group compared with the Cd-treated group ($P < 0.05$, Figure 4d); furthermore, in the former group, the expression of miR-363-3p was suppressed (Figure 4d) and the expression of KLF4 was significantly upregulated (both $P < 0.05$, Figure 4d-4f). In addition, overexpression of hsa_circ_0075684 suppressed the upregulation of Fn and α-SMA and promoted the upregulation of E-Cad in response to cadmium exposure (all $P < 0.05$, Figure 4e and 4f). The above results indicated that the overexpression of hsa_circ_0075684 alleviated cadmium-induced renal fibrosis by downregulating the expression of miR-363-3p.

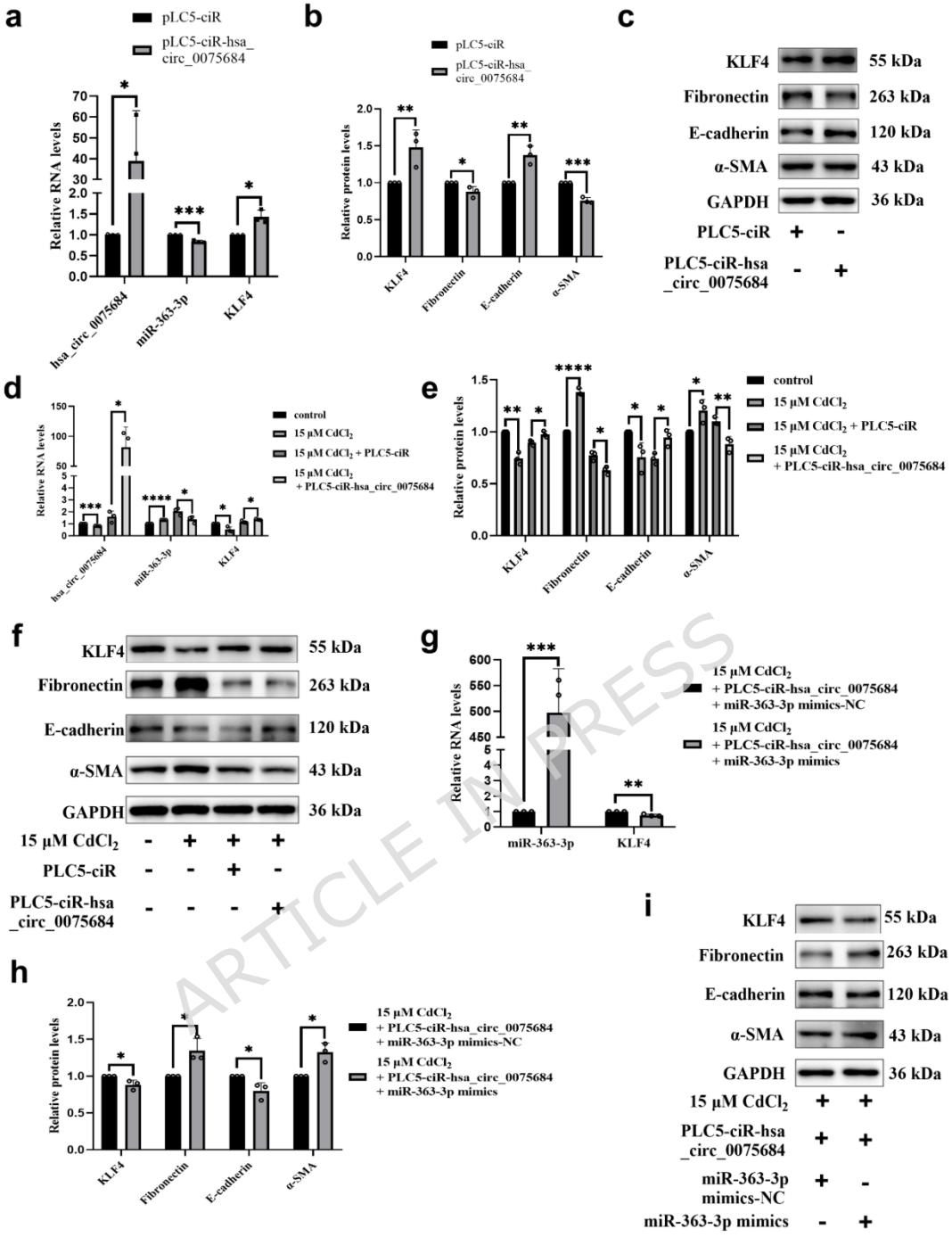

Figure 4. Effects of overexpression of hsa_circ_0075684, overexpression of miR-363-3p and treatment with cadmium on the expression of hsa_circ_0075684, miR-363-3p, KLF4 and fibrosis indicators in HK-2 cells. (a) Relative RNA Expression of hsa_circ_0075684, miR-363-3p and KLF4 in HK-2 cells after treatment with pLC5-ciR-hsa_circ_0075684. (b, c) Relative protein expression of KLF4 and fibrosis-related proteins in HK-2 cells after treatment

with pLC5-ciR-hsa_circ_0075684. (d) Relative RNA expression of hsa_circ_0075684, miR-363-3p and KLF4 in HK-2 cells after treatment with 15 μM $CdCl_2$+pLC5-ciR-hsa_circ_0075684. (e, f) Relative protein expression of KLF4 and fibrosis-related proteins in HK-2 cells after treatment with 15 μM $CdCl_2$+pLC5-ciR-hsa_circ_0075684. (g) Relative RNA expression of miR-363-3p and KLF4 in HK-2 cells after treatment with 15 μM $CdCl_2$+pLC5-ciR-hsa_circ_0075684+miR-363-3p mimics. (h, i) Relative protein expression of KLF4 and fibrosis-related proteins in HK-2 cells after treatment with 15 μM $CdCl_2$+pLC5-ciR-hsa_circ_0075684+miR-363-3p mimics. Each experiment was repeated at least three times. (n= 3 / each group, *$P < 0.05$, **$P < 0.01$, ***$P < 0.001$, ****$P < 0.0001$)

To further validate the effect of hsa_circ_0075684 on miR-363-3p, we repeated our experiments and constructed cell models of hsa_circ_0075684 and miR-363-3p overexpression. The results showed that miR-363-3p expression was upregulated in the Cd+pLC5-ciR-hsa_circ_0075684+miR-363-3p mimics-treated group compared with the Cd+pLC5-ciR-hsa_circ_0075684+miR-363-3p mimics NC group ($P < 0.05$, Figure 4g), while the expression of KLF4 was decreased ($P < 0.05$, Figure 4g-4i). In addition, the expression of Fn and α-SMA was upregulated and that of E-Cad was downregulated in the former group (all $P < 0.05$, Figure 4h and 4i). The above results indicated that overexpression of miR-363-3p could reverse the alleviating effect of hsa_circ_0075684 on cadmium-induced renal fibrosis.

Construction of a subchronic cadmium-induced renal fibrosis model in mice

In this study, a model of cadmium-induced renal fibrosis was successfully

established in C57BL/6 mice via gavage with different concentrations of a $CdCl_2$ dye solution for 90 days. After dissecting the mice and fixing the kidneys, tissue sections were stained according to Masson's staining to evaluate renal fibrosis. The results showed that the renal tissues from the control group were morphologically well organised, with normal glomeruli and interstitium; in contrast, fibrosis was clearly observed in the renal tissues from the 5, 10 and 20 mg/kg $CdCl_2$ groups, and the fibrotic lesions were mainly in the renal interstitium ($P < 0.05$, Figure 5a and 5b). Subsequently, the expression of the fibrotic proteins Fn, α-SMA and E-Cad in renal tissues was examined via western blotting. The results showed that the expression of the pro-fibrotic proteins Fn and α-SMA was upregulated, while that of the anti-fibrotic protein E-Cad was downregulated (all $P < 0.05$); a significant dose–response relationship was observed within a certain Cd concentration range (β_{Fn}/95%confidence = 0.031/0.013 to 0.048, $\beta_{E\text{-}Cad}$/95%confidence = -0.020/-0.027 to -0.012, $\beta_{\alpha\text{-}SMA}$/95%confidence = 0.027/0.015 to 0.038, all $P < 0.05$, Figure 5d and 5e), demonstrating the successful establishment of a cadmium-induced renal fibrosis model in mice.

After completing the modelling of renal fibrosis in mice, we examined the expression of miR-363-3p and its downstream effector KLF4 in the kidneys of mice treated with different concentrations of cadmium and control mice. The results showed that the expression of miR-363-3p was elevated in the kidneys of the 20 mg/kg $CdCl_2$ treated mice compared with control mice ($t = 9.42$, $P < 0.05$, Figure 5c), whereas the expression of KLF4 mRNA and protein was decreased in the kidneys of the 20 mg/kg $CdCl_2$ treated mice compared with control mice ($t_{mRNA} = 3.875$, $t_{protein} = 3.575$, all $P < 0.05$, Figure 5c-5e). The above results further validated the results of the in vitro experiments, showing that cadmium exposure induced the upregulation of miR-363-3p and downregulation of KLF4 expression.

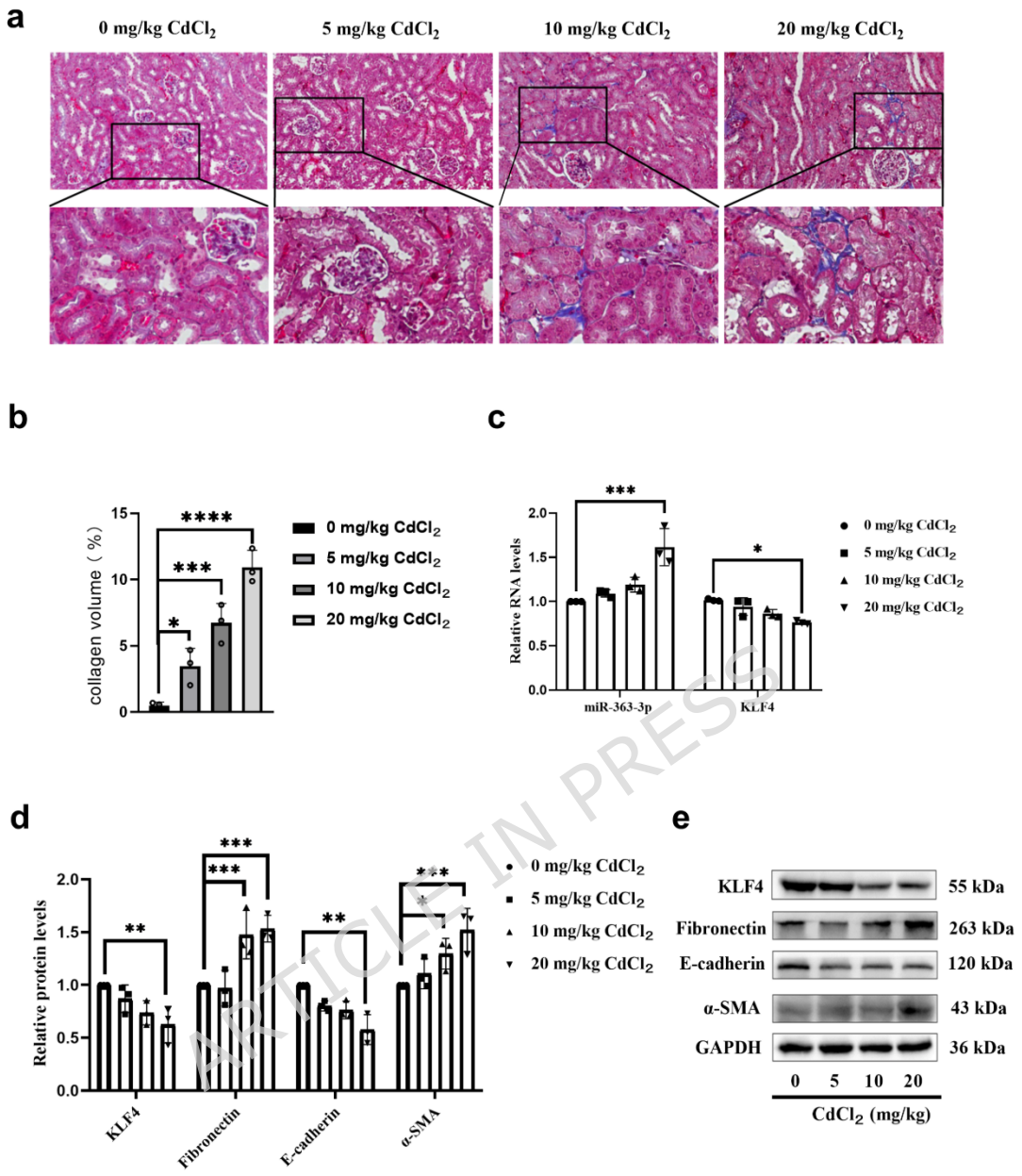

Figure 5. Construction of a subchronic cadmium-induced renal fibrosis model in mice. (a) Masson-stained kidney tissues from mice treated with different cadmium concentrations. (b) Quantified analysis result of masson-stained kidney tissues from mice treated with different cadmium concentrations. (c) Relative RNA expression of miR-363-3p and KLF4 in renal tissues from mice treated with different cadmium concentrations. (d, e) Relative protein expression of KLF4 and fibrosis-related proteins in renal tissues from mice treated with different cadmium concentrations. Each experiment was repeated at least three

times. (n= 3 / each group, *$P < 0.05$, **$P < 0.01$, ***$P < 0.001$, ****$P < 0.0001$)

Discussion

Both national and international agencies have sought to regulate exposure to cadmium in response to increasing evidence of its toxicity [36]. For example, the permissible limit of exposure to cadmium-Time Weighted Average Permition Exposure Limit is 0.005 mg/m3 (fumes) in USA, 0.05 mg/m3 (fumes) in Japan and 0.01 mg/m3 (fumes) in China [37-39]. The World Health Organisation has suggested a tolerable weekly cadmium intake limit of 7 μg/kg/body weight/week [40]. Given these limitations, humans' exposure to cadmium is mostly long-term and low-level. However, it might not be harmless to human health.

As early as 2003, Brzoska et al. [41] developed animal models of Cd exposure via the drinking water (5 and 50 mg Cd/L for 24 weeks); through experiments, they found that Cd caused structural and functional kidney damage even at a relatively low levels (5 mg/L) corresponding to human environmental exposure. In our study, we constructed animal models via the intragastric administration of cadmium at doses of 0, 5, 10 and 20 mg/kg for 90 days; here, 20 mg/kg was equal to treatment with drinking water containing 50 mg Cd/L. After 90 days of intragastric Cd administration, we observed clear renal fibrosis in the renal interstitium of mice in the 20 mg/kg Cd group, thus more rapidly observing evidence of renal toxicity than that observed by Brzoska et al. [41].

In an epidemiological study, Pietro Manuel Ferraro et al. [42] found that in the U.S. population, people with urinary cadmium levels greater than 0.001 mg/L or blood cadmium levels greater than 0.0006 mg/L had an increased risk of developing CKD. Kaneda et al. [43] found that in the Japanese population, a higher serum cadmium concentration was significantly and positively associated with systolic blood pressure and diastolic blood pressure and hypertension prevalence.

Both animal and epidemiological studies have suggested that the cadmium exposure limits set previously by national and international agencies may not have been sufficient to protect the health of humans, especially workers, from cadmium toxicity [44]. Therefore, it is crucial to prevent damage caused by cadmium exposure.

To increase primary care providers' knowledge of hazardous substances in the environment and assist with the evaluation and treatment of potentially exposed patients, in 2023, the Agency for Toxic Substances and Disease Registry provided a case study on cadmium (https://www.atsdr.cdc.gov/csem/cadmium/cover-page.html)[45], reporting that chronic cadmium exposure affects the kidneys primarily and the bones secondarily [45]. Thus, the prevention of kidney injury is a primary objective of preventing chronic cadmium toxicity. However, cadmium-induced CKD involves a complex and extensive gene regulatory network, which remains a puzzle.

In our study, we confirmed the crucial involvement of a novel signaling pathway, hsa_circ_0075684/miR-363-3p/KLF4, in the gene regulatory network associated with cadmium-induced CKD through both *in vivo* and *in vitro* experiments. In our previous study, we found that the miR-363-3p/PI3K signaling pathway regulated apoptosis in response to cadmium-induced renal injury [9]. Our findings suggest that a huge but incompletely understood regulatory network centred around miR-363-3p plays a role in cadmium-induced CKD. However, additional in-depth research is needed. Notably, miR-363-3p is known to play roles in cancer, neonatal hypoxic–ischemic encephalopathy, gastric mucosal injury, polycystic ovary syndrome and other conditions [46-49]. It is involved in several signaling pathways, including the miR-363-3p/DKK3, miR-363-3p/DUSP5 and miR-363-3p/DUSP10 pathways [46-49]. Futhermore, some researchers found that PI3K/AKT signaling was activated by KLF4[50,51], which may suggest a potential axis, hsa_circ_0075684/miR-363-3p/KLF4/PI3K, play a role in cadmium-

induced CKD, while needing further study. In addition, KLF4 can act as a transcriptional repressor of profibrotic genes, potentially serving as a negative regulator downstream of or parallel to the TGF-β/Smad axis[52]. These observations may suggest exploration of the roles of those signaling pathways in cadmium-induced CKD, thus completing the gene regulatory network centred around miR-363-3p.

Our study has several strengths. First, we conducted a bioinformatics analysis using six databases, namely a database of genes regulated by chemical substances (CTD), a database of normal human tissue gene expression (GTEx), three microRNA databases (miRDB, miRWalk and TarBase) and a famous circular RNA database (starBase), to search for potential signaling pathways involved in cadmium-induced CKD, which was effective and yielded precise results (the stringent multi-database intersection minimized noise from single-source biases). Second, our research revealed the crucial role of a novel signaling pathway in cadmium-induced CKD and suggested that the huge associated regulatory network may be centred around miR-363-3p. Nevertheless, our study also has some limitations. First, we did not explore the predicted value of cadmium-induced CKD and lack of clinical validation. Second, small animals (n=3/ each group) increased risk of Type II error. Third, no mechanistic link to Cd uptake. Fourth, due to species differences, the mice model lacks data of hsa_circ_0075684, thus weakens the claim that the entire pathway is functional in vivo.

Although exploring the mechanism of cadmium-induced CKD will be a long process, it eventually will be elucidated via the gradual accumulation of research. The findings will play a role in preventing cadmium toxicity.

Materials and methods

Bioinformatic analysis

Predicting of miR-363-3p downstream target genes with miRNA databse: miRDB (version 6.0) (https://mirdb.org/), miRWalk (version 3.0) (http://mirwalk.umm.uni-heidelberg.de/) and Tarbase (version 7.0) (http://www.microrna.gr/tarbase). In order to reduce false negative and false positive, we got 102 downstream target genes by intersecting the prediction results from the three databases (Supplementary Table 3 and Supplementary Figure 1). Predicting of miR-363-3p upstream target genes with Starbase (version 2.0) (https://rnasysu.com/encori/).

CTD was use to search cadmium-related genes that potential regulated by miR-363-3p. We search the cadmium-related genes by three criteria, mRNA or protein decreased by cadmium, experimental confirmation in human cells until August, 2022. And we got 929 genes related to cadmium.

GO enrichment analysis and KEGG enrichment analysis were performed by R script (version 4.3.1) using 'clusterProfiler' package to analyze miR-363-3p's predicted downstream genes enrichment pathway. Permission has been obtained from Kanehisa laboratories for using KEGG pathway database[53].

We downloaded gene expression profile of kidney from GTEx until August, 2022. To remove genes with low expression values, the following steps were applied. First, Transcripts per million (TPM) values <1 were considered unreliable and substituted with zero. Second, genes expressed in <10% of all kidney samples were removed. Finally, a total of 16358 kidney-relative genes were used for next filter [54].

Cell culture and treatment

HK-2 cells (human proximal tubule epithelial cell, passage 2) were donated by Professor Wang Qing (School of Public Health, Sun Yat-sen University, China). HK-2 cells were cultured in DMEM/F12 10 % which includes 10% foetal bovine serum and 1% Penicillin-Streptomycin Solution and incubated at 37°C with 5 %

CO2 in incubator until passage 8. HK-2 cells (passage 3 to passage 8) were treatment in a range of concentrations of $CdCl_2$ (Sigma-Aldrich, USA) diluted with deionized water for 48 h based on our previous study [9].

Cell viability assay

The Cell viability assay was performed by the CCK-8 assay kit (Dojindo, Japan). HK-2 cells were seeded in 96-well plates and treated with 0, 5, 10, 20, 40 or 80 mM $CdCl_2$ for 48 h. After 48 h of incubation, add 100 μL of mixture to each well (100 μL of cell complete medium for every 10 μL of CCK-8 reagent), and put it into the incubator to react for 2 h. and then absorbances were measured at 450 nm on a microplate reader.

Dual-luciferase reporter gene assay

HK-2 cells were seeded in 96-well plate and cotransfected with the corresponding psiCHECK-2-KLF4 WT/MUT vector, psiCHECK-2-hsa_circ_0075684 WT/MUT vector and miR363-3p mimics NC/mimics for 24 h (Because the cytotoxicity of co-transfection at 48 h was too high, 24 h was chosen instead.). Subsequently, the relative luciferase activity was measured using a Dual-Luciferase Reporter Assay Kit (Promega, USA) on a microplate reader. The sequence of psiCHECK-2-KLF4 WT/MUT vector and psiCHECK-2-hsa_circ_0075684 WT/MUT vector are as follow: UGAAUUGUGUAUUGAUGCAAUAU (psiCHECK-2-KLF4 WT), UGAAUUGUGUAUUGAAU (psiCHECK-2-KLF4 MUT), CCUAGAUGACCUUAUCGGGUGCAAUA (psiCHECK-2-hsa_circ_0075684 WT), CCUACCUUGGA (psiCHECK-2-hsa_circ_0075684 MUT).

Cell transfection

Transfections were performed using riboFECT CP Transfection Kit (Ribobio, Guangzhou, China) for miR-363-3p and KLF4 or jetPRIME Buffer (Polyplus,

France) for hsa_circ_0075684 according to the manufacturer's instructions. HK-2 cells were seeded at a density of 2.0 × 10^5 cells per well in 6-well plates and grown to 50-60 % confluence. And then co-transfected with the corresponding 50 nM miR363-3p mimics NC/mimics, 100 nM miR363-3p inhibitor NC/inhibitor or 50 nM si-*KLF4* or 2 μg plasmid of pLC5-ciR-hsa_circ_0075684 for 48 h. Subsequently, the cells were collected for subsequent experiments. The target sequence of si-*KLF4* is as follow: GACCAGGCACTACCGTAAA. The sequence of pLC5-ciR-hsa_circ_0075684 is shown in supplementary Table 6.

RNA isolation and RT-qPCR

Total RNA was extracted using RNAex Pro RNA Extraction Reagent (Accurate Biology, Hunan, China), and total RNA was converted to cDNA using Evo M-MLV Reverse Transcription Kit/II (Accurate Biology, Hunan, China) or miRcute Enhanced miRNA cDNA First-Strand Synthesis Kit (TianGen, Beijin, China). then, RT-qPCR was performed using SYBR Green Realtime PCR Master Mix kit (Accurate Biology, Hunan, China). The thermal cycling conditions were as follows: initial denaturation at 95 ºC for 30 second; followed by 40 cycles of 95 ºC for 5 second and 60 ºC for 30 second. The relative changes in KLF4, miR-363-3p, and hsa_circ_0075684 expression were determined by calculating $2^{-\Delta\Delta Ct}$ values. Using GAPDH as an internal reference for KLF4 and hsa_circ_0075684 expression detection, and using U6 as an internal reference for miR-363-3p expression detection based on our previous study [9]. The sequences of specific primers (Synbio Technologies, Suzhou, China) used for qRT-PCR are shown in Supplementary Table 1.

Western blot

Total protein was extracted with lysate (Beyotime, Shanghai, China), and protein quantification was performed with BCA protein concentration assay kit

(NCM Biotech, Suzhou, China). Equal amounts of protein (15 μg for cellular proteins and 20 μg for tissue extracts) were separated by 10% dodecyl polyacrylamide gel electrophoresis, then transferred to PVDF membrane and closed with rapid closure solution for 30 min at room temperature, then incubated with primary antibody overnight at 4°C and secondary antibody at room temperature for 2h, finally, protein imaging was performed using a Tanon-5200CE chemiluminescent imaging system (Tanon, Shanghai, China) and a Key GEN BioTECH ECL detection kit (GenXion, Guangzhou, China). The expression levels of the measured proteins were normalized to GAPDH and the images were quantified using ImageJ software (version 1.46, NIH, Maryland, USA). Primary antibodies used in the study were as follows: anti-α-SMA (1:2000, proteintech); anti Fibronectin (1:5000, proteintech); anti-E-cadherin (1:2000, proteintech); anti-KLF4 (1:2000, proteintech); and anti-GAPDH (1:8000, proteintech).

Animal models

All methods were carried out in accordance with relevant guidelines and regulations. All methods were reported in accordance with ARRIVE guidelines. Twelve healthy pathogen-free (SPF) 6-week-old C57BL/6J female mice were purchased from Guangdong Medical Animal Center and raised in isolation for 7 days. Mice were housed in standard specific pathogen-free conditions within a barrier facility and were maintained under a controlled 12-hour light/dark cycle (lights on at 8:00 AM) at a temperature of 20 to 25 °C and a relative humidity of 40 to 70 %. According to the animal experimental dose (50 mg/L) in the high background area of the environment and the daily drinking water of mice[41], 50 mg/L was converted into the highest dose of intragastric administration, an 6-week-old C57BL/6J female mice drank approximately 8 ml per day and the weight was about 20 g (based on previous study [55,56] and our experimental experience), The highest intragastric administration were calculated using the following formula: 50 mg/L ×0.008 L（equal to 8 mL）/ 0.02 kg (equal to 20 g) =

20 mg/kg. The body weight of mice was randomly divided into 4 groups (three mice each group) according to the method of random number table, which were 0 mg/kg, 5 mg/kg, 10 mg/kg and 20 mg/kg respectively. The intragastric dose was 10 mL/kg for 90 days. At the end of the experiment, the mice were euthanized by cervical dislocation after isoflurane (MedChemExpress, USA) anesthesia. This animal experiment was approved by *Animal Experiment Ethics Committee of Guangdong Occupational Disease Prevention and Control Institute* and the approval number of laboratory animal ethics is GDHODAEC2023030.

Masson staining

Mice kidneys were collected and immediately immersed in 4% paraformaldehyde overnight, followed by tissue embedding. The embedded tissues were cut into 4 μm thick sections and stained with Solepol Masson Trichrome Staining Kit (Solarbio, Beijing, China), followed by multiple dehydration, xylene clearing, neutral gum sealing, and finally, the collagen fibers in the mice kidney tissues were observed in blue staining under a light microscope. The images were quantified using ImageJ software.

Statistical analysis

GraphPad Prism 8.0 was used for analysis and graphing, and data were expressed as" means ± standard deviation ($\bar{X} \pm$ SD)". The *t*-test was used to compare the differences in means between the two groups, the Oneway-ANOVA was used to compare the differences between multiple groups (> 2 groups), and the LSD method was used to compare two groups. If > 3 groups, the Boferroni method is used instead. Linear regression was used for dose-response. Differences were considered statistically significant at $P < 0.05$ (two-sided test).

Acknowledgements

Professional English language editing support was provided by AsiaEdit

(asiaedit.com).

CRediT authorship contribution statement

YiQi Huang: Writing – original draft, Visualisation, Methodology, Investigation, Formal analysis. Jiazhen Zhou: Writing – review & editing, Project administration, Methodology, Investigation, Formal analysis, Conceptualisation. Lili Liu: Supervision, Funding acquisition, Conceptualisation. Guoliang Li, Zhiqiang Zhao and Yaotang Deng: Writing – review & editing, Investigation. Siming Xian, Yue Hu and Mushi Yi: Writing – review & editing, Investigation, Conceptualisation.

Declaration of Competing Interest

The authors declare no conflicts of interest.

Funding Declaration

This research was supported by the National Natural Science Foundation of China (No. 81972990), Key Scientific Research Project Fund of GDHOD (Z2022-13 and Z2023-07).

Data availability

All data used and/or analysed during the current study available from the corresponding author on reasonable request. E-mail: lli257@163.com.

References

1 Peana, M. *et al.* Biological Effects of Human Exposure to Environmental Cadmium. *Biomolecules* **13**, doi:10.3390/biom13010036 (2022).

2 Rafati R, M., Kazemi, S. & Moghadamnia, A. A. Cadmium toxicity and treatment: An update. *Caspian journal of internal medicine* **8**, 135-145, doi:10.22088/cjim.8.3.135 (2017).

3 Zeng, T. *et al.* Urinary metabolic characterization with nephrotoxicity for residents under cadmium exposure. *Environment international* **154**, 106646, doi:10.1016/j.envint.2021.106646 (2021).

4 Charkiewicz, A. E., Omeljaniuk, W. J., Nowak, K., Garley, M. & Nikliński, J. Cadmium Toxicity and Health Effects-A Brief Summary. *Molecules (Basel, Switzerland)* **28**, doi:10.3390/molecules28186620 (2023).

5 Gao, H. *et al.* Combination Effect of Microcystins and Arsenic Exposures on CKD: A Case-Control Study in China. *Toxins* **15**, doi:10.3390/toxins15020144 (2023).

6 Hernández-Cruz, E. Y., Amador-Martínez, I., Aranda-Rivera, A. K., Cruz-Gregorio, A. & Pedraza Chaverri, J. Renal damage induced by cadmium and its possible therapy by mitochondrial transplantation. *Chemico-biological interactions* **361**, 109961, doi:10.1016/j.cbi.2022.109961 (2022).

7 Collaboration, G. C. K. D. Global, regional, and national burden of chronic kidney disease, 1990-2017: a systematic analysis for the Global Burden of Disease Study 2017. *Lancet (London, England)* **395**, 709-733, doi:10.1016/s0140-6736(20)30045-3 (2020).

8 Kalantar-Zadeh, K., Jafar, T. H., Nitsch, D., Neuen, B. L. & Perkovic, V. Chronic kidney disease. *Lancet (London, England)* **398**, 786-802, doi:10.1016/s0140-6736(21)00519-5 (2021).

9 Chen, J. *et al.* MicroRNA-363-3p promotes apoptosis in response to cadmium-induced renal injury by down-regulating phosphoinositide 3-kinase expression. *Toxicology letters* **345**, 12-23, doi:10.1016/j.toxlet.2021.04.002 (2021).

10 Dong, S. *et al.* MicroRNA-363-3p downregulation in papillary thyroid cancer inhibits tumor progression by targeting NOB1. *Journal of investigative medicine : the official publication of the American Federation for Clinical Research* **69**, 66-74, doi:10.1136/jim-2020-001562 (2021).

11 Li, Y. *et al.* Oncogenic cAMP responsive element binding protein 1 is overexpressed upon loss of tumor suppressive miR-10b-5p and miR-363-3p in renal cancer. *Oncology reports* **35**, 1967-1978, doi:10.3892/or.2016.4579 (2016).

12 Zhang, Y. *et al.* CircCTNNA1 acts as a ceRNA for miR-363-3p to facilitate the progression of colorectal cancer by promoting CXCL5 expression. *Journal of biological research (Thessalonike, Greece)* **28**, 7, doi:10.1186/s40709-021-00135-8 (2021).

13 Li, L. *et al.* Oxidatively stressed extracellular microenvironment drives fibroblast activation and kidney fibrosis. *Redox biology* **67**, 102868, doi:10.1016/j.redox.2023.102868 (2023).

14 Yang, Z., He, Y., Ma, Q., Wang, H. & Zhang, Q. Alleviative effect of melatonin against the nephrotoxicity induced by cadmium exposure through regulating renal oxidative stress, inflammatory reaction, and fibrosis in a mouse model. *Ecotoxicology and environmental safety* **265**, 115536, doi:10.1016/j.ecoenv.2023.115536 (2023).

15 Joardar, S. *et al.* Rosmarinic Acid Attenuates Cadmium-Induced Nephrotoxicity via Inhibition of Oxidative Stress, Apoptosis, Inflammation and Fibrosis. *International journal of molecular sciences* **20**, doi:10.3390/ijms20082027 (2019).

16 Dong, X., Li, Y., Cao, R. & Xu, H. MicroRNA-363-3p Inhibits the Expression of Renal Fibrosis Markers in TGF-β1-Treated HK-2 Cells by Targeting TGF-β2. *Biochemical genetics* **59**, 1033-1048, doi:10.1007/s10528-021-10044-z (2021).

17 Tian, Y. *et al.* Bioinformatics Analysis of Key Genes and circRNA-miRNA-mRNA Regulatory Network in Gastric Cancer. *BioMed research international* **2020**, 2862701, doi:10.1155/2020/2862701 (2020).

18 Sharma, R., Kaur, G., Bansal, P., Chawla, V. & Gupta, V. Bioinformatics Paradigms in Drug Discovery and Drug Development. *Current topics in medicinal chemistry* **23**, 579-588, doi:10.2174/1568026623666221229113456 (2023).

19 Deng, S. *et al.* Selecting Hub Genes and Predicting Target Genes of microRNAs in Tuberculosis via the Bioinformatics Analysis. *Genetics research* **2021**, 6226291, doi:10.1155/2021/6226291 (2021).

20 Chen, Y. & Wang, X. miRDB: an online database for prediction of functional microRNA targets. *Nucleic acids research* **48**, D127-d131, doi:10.1093/nar/gkz757 (2020).

21 Sticht, C., De La Torre, C., Parveen, A. & Gretz, N. miRWalk: An online resource for prediction of microRNA binding sites. *PloS one* **13**, e0206239, doi:10.1371/journal.pone.0206239 (2018).

22 Skoufos, G. *et al.* TarBase-v9.0 extends experimentally supported miRNA-gene interactions to cell-types and virally encoded miRNAs. *Nucleic acids research* **52**, D304-d310, doi:10.1093/nar/gkad1071 (2024).

23 Li, J. H., Liu, S., Zhou, H., Qu, L. H. & Yang, J. H. starBase v2.0: decoding miRNA-ceRNA, miRNA-ncRNA and protein-RNA interaction networks from large-scale CLIP-Seq data. *Nucleic acids research* **42**, D92-97, doi:10.1093/nar/gkt1248 (2014).

24 Wyatt, B. *et al.* Transforming environmental health datasets from the comparative toxicogenomics database into chord diagrams to visualize molecular mechanisms. *Frontiers in toxicology* **6**, 1437884, doi:10.3389/ftox.2024.1437884 (2024).

25 Carithers, L. J. & Moore, H. M. The Genotype-Tissue Expression (GTEx) Project. *Biopreservation and biobanking* **13**, 307-308, doi:10.1089/bio.2015.29031.hmm (2015).

26 He, Z., He, J. & Xie, K. KLF4 transcription factor in tumorigenesis. *Cell death discovery* **9**, 118, doi:10.1038/s41420-023-01416-y (2023).

27 Zhao, J., Wang, X., Wu, Y. & Zhao, C. Krüppel-like factor 4 modulates the miR-101/COL10A1 axis to inhibit renal fibrosis after AKI by regulating epithelial-mesenchymal transition. *Renal failure* **46**, 2316259, doi:10.1080/0886022x.2024.2316259 (2024).

28 Chandran, R. R. *et al.* Distinct roles of KLF4 in mesenchymal cell subtypes during lung fibrogenesis. *Nature communications* **12**, 7179, doi:10.1038/s41467-021-27499-8 (2021).

29 Shi, Y. Y., Ma, Y. H., Zhang, R. & Li, R. S. Downregulation of miR-34a ameliorates inflammatory response and apoptosis induced by renal ischemia-reperfusion by promoting Kruppel-like factor 4 expression. *European review for medical and pharmacological sciences* **24**, 11683-11689, doi:10.26355/eurrev_202011_23813 (2020).

30 Yang, X., Li, B., Guan, Y. & Jiang, H. M. Expressions and related mechanisms of miR-212 and KLF4 in rats with acute kidney injury. *Molecular and cellular biochemistry* **476**, 1741-1749, doi:10.1007/s11010-020-04016-x (2021).

31 Shi, N. & Chen, S. Y. Mechanisms simultaneously regulate smooth muscle

proliferation and differentiation. *Journal of biomedical research* **28**, 40-46, doi:10.7555/jbr.28.20130130 (2014).

32 Fang, X. D. *et al.* MiR-449a downregulation alleviates the progression of renal interstitial fibrosis by mediating the KLF4/MFN2 axis. *International urology and nephrology* **55**, 1837-1846, doi:10.1007/s11255-023-03503-6 (2023).

33 Mreich, E., Chen, X. M., Zaky, A., Pollock, C. A. & Saad, S. The role of Krüppel-like factor 4 in transforming growth factor-β-induced inflammatory and fibrotic responses in human proximal tubule cells. *Clinical and experimental pharmacology & physiology* **42**, 680-686, doi:10.1111/1440-1681.12405 (2015).

34 Liu, J. *et al.* CircRNA circ-ITCH improves renal inflammation and fibrosis in streptozotocin-induced diabetic mice by regulating the miR-33a-5p/SIRT6 axis. *Inflammation research : official journal of the European Histamine Research Society ... [et al.]* **70**, 835-846, doi:10.1007/s00011-021-01485-8 (2021).

35 Zhou, W. *et al.* circPlekha7 suppresses renal fibrosis via targeting miR-493-3p/KLF4. *Epigenomics* **14**, 199-217, doi:10.2217/epi-2021-0370 (2022).

36 Satoh, M., Koyama, H., Kaji, T., Kito, H. & Tohyama, C. Perspectives on cadmium toxicity research. *The Tohoku journal of experimental medicine* **196**, 23-32, doi:10.1620/tjem.196.23 (2002).

37 Stamatis, N., Kamidis, N., Pigada, P., Stergiou, D. & Kallianiotis, A. Bioaccumulation Levels and Potential Health Risks of Mercury, Cadmium, and Lead in Albacore (Thunnus alalunga, Bonnaterre, 1788) from The Aegean Sea, Greece. *International journal of environmental research and public health* **16**, doi:10.3390/ijerph16050821 (2019).

38 Qing, Y. *et al.* Dose-response evaluation of urinary cadmium and kidney injury biomarkers in Chinese residents and dietary limit standards. *Environmental health : a global access science source* **20**, 75, doi:10.1186/s12940-021-00760-9 (2021).

39 Satarug, S., Vesey, D. A., Gobe, G. C. & Phelps, K. R. Estimation of health risks associated with dietary cadmium exposure. *Archives of toxicology* **97**, 329-358, doi:10.1007/s00204-022-03432-w (2023).

40 Kim, K. *et al.* Dietary Cadmium Intake and Sources in the US. *Nutrients* **11**, doi:10.3390/nu11010002 (2018).

41 Brzóska, M. M., Kamiński, M., Supernak-Bobko, D., Zwierz, K. & Moniuszko-Jakoniuk, J. Changes in the structure and function of the kidney of rats chronically exposed to cadmium. I. Biochemical and histopathological studies. *Archives of toxicology* **77**, 344-352, doi:10.1007/s00204-003-0451-1 (2003).

42 Ferraro, P. M., Costanzi, S., Naticchia, A., Sturniolo, A. & Gambaro, G. Low level exposure to cadmium increases the risk of chronic kidney disease: analysis of the NHANES 1999-2006. *BMC public health* **10**, 304, doi:10.1186/1471-2458-10-304 (2010).

43 Kaneda, M. *et al.* Low Level of Serum Cadmium in Relation to Blood Pressures Among Japanese General Population. *Biological trace element research* **200**, 67-75, doi:10.1007/s12011-021-02648-8 (2022).

44 Satarug, S. Is Chronic Kidney Disease Due to Cadmium Exposure Inevitable and Can It Be Reversed? *Biomedicines* **12**, doi:10.3390/biomedicines12040718 (2024).

45 Faroon, O. *et al.* in *Toxicological Profile for Cadmium* (Agency for Toxic Substances and Disease Registry (US), 2012).

46 Sang, M., Yu, Y., Zhou, Z., Zhang, Y. & Chang, H. Differential expression of serum mir-363-3p in patients with polycystic ovary syndrome and its predictive value for their pregnancy. *BMC women's health* **23**, 264, doi:10.1186/s12905-023-02337-9 (2023).

47 Zongdan, J. *et al.* The mechanism of miR-363-3p/DUSP10 signaling pathway involved in the gastric mucosal injury induced by clopidogrel. *Toxicology mechanisms and methods* **31**, 150-158, doi:10.1080/15376516.2020.1850960 (2021).

48 Jia, Y. *et al.* MiR-363-3p attenuates neonatal hypoxic-ischemia encephalopathy by targeting DUSP5. *Neuroscience research* **171**, 103-113, doi:10.1016/j.neures.2021.03.003 (2021).

49 Xu, L. Z., Ning, J. Z., Ruan, Y. & Cheng, F. MiR-363-3p promotes prostate cancer tumor progression by targeting Dickkopf 3. *Journal of clinical laboratory analysis* **36**, e24360, doi:10.1002/jcla.24360 (2022).

50 Xiong, J. M. *et al.* Curcumin nicotinate suppresses abdominal aortic aneurysm pyroptosis via lncRNA PVT1/miR-26a/KLF4 axis through regulating the PI3K/AKT signaling pathway. *Toxicology research* **10**, 651-661, doi:10.1093/toxres/tfab041 (2021).

51 Sekita, Y. *et al.* AKT signaling is associated with epigenetic

reprogramming via the upregulation of TET and its cofactor, alpha-ketoglutarate during iPSC generation. *Stem cell research & therapy* **12**, 510, doi:10.1186/s13287-021-02578-1 (2021).

52 Ghaleb, A. M. & Yang, V. W. Krüppel-like factor 4 (KLF4): What we currently know. *Gene* **611**, 27-37, doi:10.1016/j.gene.2017.02.025 (2017).

53 Kanehisa, M., Furumichi, M., Sato, Y., Matsuura, Y. & Ishiguro-Watanabe, M. KEGG: biological systems database as a model of the real world. *Nucleic acids research* **53**, D672-D677, doi:10.1093/nar/gkae909 (2025).

54 Chung, W. *et al.* Single-cell RNA-seq enables comprehensive tumour and immune cell profiling in primary breast cancer. *Nature communications* **8**, 15081, doi:10.1038/ncomms15081 (2017).

55 Claassen, V. in *Techniques in the Behavioral and Neural Sciences* Vol. 12 (ed V. Claassen) 267-287 (Elsevier, 1994).

56 Bachmanov, A. A., Reed, D. R., Beauchamp, G. K. & Tordoff, M. G. Food Intake, Water Intake, and Drinking Spout Side Preference of 28 Mouse Strains. *Behavior Genetics* **32**, 435-443, doi:10.1023/A:1020884312053 (2002).

Table

Table 1. Top 10 results for the prediction of circRNAs that regulate miR-363-3p

circBase ID	Gene ID	Gene Type	Gene Name	Clip Exp Num
hsa_circ_0075684	NM_013262	circRNA	*MYLIP*	50
hsa_circ_0051279	NM_015125	circRNA	*CIC*	50
hsa_circ_0020013	NM_004419	circRNA	*DUSP5*	49
hsa_circ_0016068	NM_006763	circRNA	*BTG2*	46
hsa_circ_0084491	NM_052937	circRNA	*PCMTD1*	46
hsa_circ_0014033	NM_021960	circRNA	*MCL1*	45
hsa_circ_0078229	NM_198887	circRNA	*NUP43*	44
hsa_circ_0029555	NM_005895	circRNA	*GOLGA3*	44
hsa_circ_0013997	NM_030920	circRNA	*ANP32E*	43
hsa_circ_ 0067979	NM_022763	circRNA	*FNDC3B*	42